DOI: 10.1002/chem.200701335

Single-Step Electron Transfer on the Nanometer Scale: Ultra-Fast Charge Shift in Strongly Coupled Zinc Porphyrin–Gold Porphyrin Dyads

Jérôme Fortage,[a] Julien Boixel,[a] Errol Blart,[a] Leif Hammarström,*[b] Hans Christian Becker,*[b] and Fabrice Odobel*[a]

Abstract: The synthesis, electrochemical properties, and photoinduced electron transfer processes of a series of three novel zinc(II)–gold(III) bisporphyrin dyads ($ZnP{-}S{-}AuP^{+}$) are described. The systems studied consist of two trisaryl porphyrins connected directly in the *meso* position via an alkyne unit to *tert*-(phenylenethynylene) or penta(phenylenethynylene) spacers. In these dyads, the estimated center to center interporphyrin separation distance varies from 32 to 45 Å. The absorption, emission, and electrochemical data indicate that there are strong electronic interactions between the linked elements, thanks to the direct attachment of the spacer on the porphyrin ring through the alkyne unit. At room temperature in toluene, light excitation of the zinc porphyrin results in almost quantitative formation of the charge shifted state $^{\bullet+}ZnP{-}S{-}AuP^{\bullet}$, whose lifetime is in the order of hundreds of picoseconds. In this solvent, the charge-separated state decays to the ground state through the intermediate population of the zinc porphyrin triplet excited state. Excitation of the gold porphyrin leads instead to rapid energy transfer to the triplet ZnP. In dichloromethane the charge shift reactions are even faster, with time constants down to 2 ps, and may be induced also by excitation of the gold porphyrin. In this latter solvent, the longest charge-shifted lifetime ($\tau =$ 2.3 ns) was obtained with the penta(phenylenethynylene) spacer. The charge shift reactions are discussed in terms of bridge-mediated super-exchange mechanisms as electron or hole transfer. These new bis-porphyrin arrays, with strong electronic coupling, represent interesting molecular systems in which extremely fast and efficient long-range photoinduced charge shift occurs over a long distance. The rate constants are two to three orders of magnitude larger than for corresponding $ZnP{-}AuP^{+}$ dyads linked via *meso*-phenyl groups to oligo-phenyleneethynylene spacers. This study demonstrates the critical impact of the attachment position of the spacer on the porphyrin on the electron transfer rate, and this strategy can represent a useful approach to develop molecular photonic devices for long-range charge separations.

Keywords: electron transfer · femtosecond spectroscopy · gold · molecular wires · porphyrinoids · zinc

Introduction

The development of molecular systems for long-range charge separation has attracted considerable attention over the past decades. One driving force for the growing interest in this area is the realization that such molecular devices can be used for a variety of applications, ranging from solar energy conversion (artificial photosynthesis and photovoltaic) to molecular electronics.

Generally, the devices designed for light-induced charge separation are composed of donors and acceptors covalently linked via a molecular spacer.[1–7] The development of appropriate spacers to promote electronic coupling is an important issue from the viewpoint of keeping a high rate of electron transfer while increasing the distance between the donor and the acceptor. Extensive theoretical analyses have been devoted to this problem,[1,2,8] but surprisingly there are few molecular devices for photoinduced charge separation

[a] Dr. J. Fortage, J. Boixel, Dr. E. Blart, Dr. F. Odobel
Université de Nantes, Nantes Atlantique Universités
CNRS
Faculté des Sciences et des Techniques
Laboratoire de Synthèse Organique (LSO), UMR CNRS 6513
2, rue de la Houssinière - BP 92208–44322 Nantes Cedex 3 (France)
Fax: (+33) 2-51-12-54-29
E-mail: Fabrice.Odobel@univ-nantes.fr

[b] Prof. L. Hammarström, Dr. H. C. Becker
Department of Photochemistry and Molecular Science
The Ångström Laboratories, Uppsala University
Regementsvägen 1, 752 37 Uppsala (Sweden)
Fax: (+46) 18-471 6844
E-mail: Leif.Hammarstrom@fotomol.uu.se
hcb@fotomol.uu.se

Supporting information for this article (synthesis of compounds, ^1H NMR spectra of the dyads **D1**–**D3** and of the compounds **25**, **27**, **29**, **31**, **32** and **33**, spectroelectrochemical data, and additional transient absorption data) is available on the WWW under http://www.chemistry.org or from the author.

that rely on the utilization of long conjugated spacers to connect the active units. Relevant examples are the *para*-(phenylenevinylene) spacers used to connect a tetracene sensitizer to a pyromellitimide acceptor described by Wasielewski and co-workers.[5] More recently the use of a similar spacer was reported by Guldi and co-workers to prepare fullerene-based dyads.[9]

In the present work, we extend a concept that we have previously reported, which involves anchoring the spacer directly on the porphyrin core to promote, in a single step, a long-range photoinduced electron transfer between porphyrin units.[10,11] In a previous investigation, we showed that the bis-ethynylenequaterthiophene spacer is suitable for promoting fast energy transfer from a zinc porphyrin to a free base porphyrin.[12] We are now interested in testing whether this concept is appropriate for photoinduced electron transfer with oligo(phenyleneethynylene) spacers. To this end, we replaced the free base porphyrin with a gold porphyrin, because the couple ZnP/AuP^+ is well suited for photoinduced charge separation. Pioneering work by Sauvage and co-workers[13] with elegant rotaxane type architectures, and more recently the groups of Albinsson and co-workers,[6,14] and Fukuzumi and co-workers,[15] have shown that efficient charge separation generally occurs in porphyrin arrays composed of zinc and gold porphyrins. Besides this, the system ZnP–S–AuP^+ offers the possibility to study the influence of the electronic properties of the spacer on the charge separation by photoexcitation of either the zinc or gold porphyrin, since both are known to bring about a charge separation. In each case, the role of the spacer can differ because the rate of the electron transfer, by a through bond mechanism, is highly dependent on the energy matching and the degree of overlap of the frontier molecular orbitals of the photoexcited chromophore and the spacer.[2,5,8,16] Furthermore, the utilization of long conjugated spacers would inevitably cause a decrease of the HOMO–LUMO gap that would therefore create an accessible π–π* state localized on the bridge. As a consequence, energy transfer from the photoexcited porphyrin to the bridge, which is in close proximity to it, could compete with electron transfer between the porphyrins. To circumvent this potential parasite reaction, phenyleneethynylene spacers appear to be better suited than oligothiophenes if one envisions using very long spacers. *para*-(Phenyleneethynylene)s are linear, relatively rigid π-conjugated molecules, and they exhibit relatively high-lying electronic excited states, even when they contain a large number of repeating units.[17]

In this work, *para*-(phenyleneethynylene)s were substituted by electron-withdrawing groups such as esters (**D1**), or by electron-donating groups such as alkoxy chains (**D2**, **D3**) (Scheme 1). These substituents were used not only to increase the solubility but also to tune the electronic properties of the bridge.

This paper focuses on the synthesis, and the electrochemical and photoinduced electron transfer of novel dyads of particular relevance to the above discussion. We show that the properties of the dyads **D1**–**D3** are not simple additions of those of their molecular components, since electronic interactions are clearly manifested in the ground and excited states. We show that attachment of a *para*-(phenyleneethynylene) spacer directly on the *meso* position of the porphyrin via a triple bond is an effective strategy to promote very fast light-induced charge separation in a single step between the porphyrins, over very long distances up to 45 Å. Indeed, light excitation of the zinc porphyrin in dyads **D1**–**D3** in dichloromethane leads to an almost quantitative electron transfer reaction from ZnP to AuP^+ on the picosecond time scale.

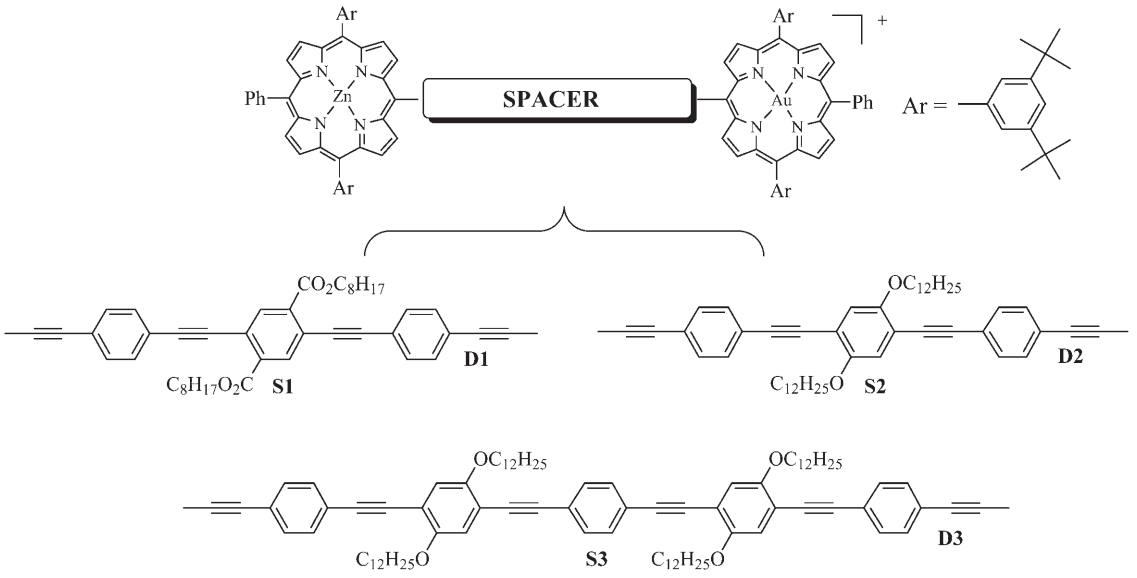

Scheme 1. Structures of the dyads at the focus of the present study.

Results and Discussion

Synthesis of the dyads: The preparation of dyads **D1**–**D3** was accomplished according to a stepwise modular approach in which the appropriate spacer is first linked to a zinc porphyrin and then to a gold porphyrin via a Sonogashira cross-coupling reaction (Scheme 2). The key building blocks for the synthesis of dyads **D1**–**D3** are the zinc iodo porphyrin **4**, the differently protected bis-ethynyl spacer **18**, **23**, and **20** and the gold halogeno porphyrin **7**, **8** (Scheme 2).

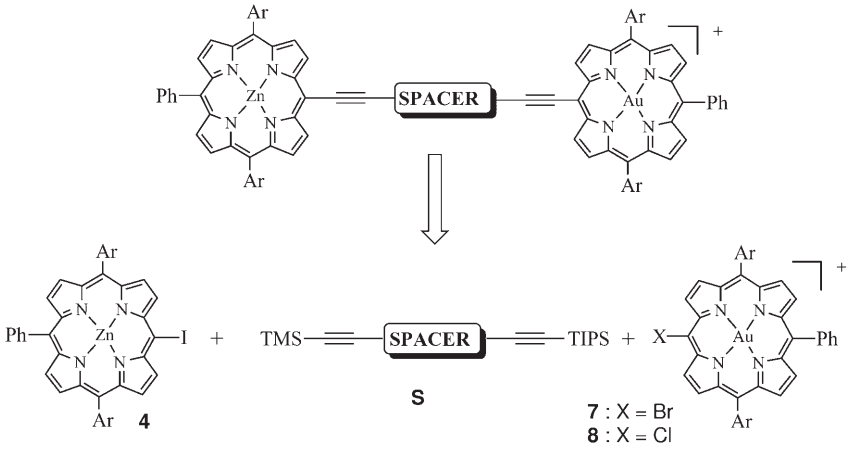

Scheme 2. Retrosynthetic strategy for the stepwise synthesis of dyads **D1**–**D3**.

Preparation of the porphyrin building blocks: Starting with the known diaryl porphyrin **1**, the third aryl group was introduced according to Senge's methodology by nucleophilic substitution of one *meso* porphyrin proton by an excess of phenyl lithium (Scheme 3).[18] This procedure presents the advantage of being simpler than our previous methods[10,12] and offers a high yield for the preparation of trisaryl porphyrin **2**. The resulting porphyrin **2** is then iodinated using bis(trifluoroacetoxy)iodobenzene at room temperature in a quantitative yield.[19] The iodoporphyrin **3** can be metallated by zinc in a 94% yield using classical conditions. Iodo gold porphyrin **6** was obtained in a modest yield (32%) using $[Au(tht)_2]SbF_6$ in refluxing chloroform in presence of lutidine (tht = tetrahydrothiophene).[20] The low yield of this reaction prompted us to test the classical conditions ($HAuCl_4$ in AcOH + AcONa)[21] but they did not give the expected porphyrin **6**, but a mixture of different decomposition by-products. Alternatively, the porphyrin **2** could be brominated with *N*-bromosuccinimide (NBS) and then submitted to gold metalation using $HAuCl_4$ in refluxing acetic acid with sodium acetate. During the reaction, the bromo group was partly substituted by a chloro group, leading to an equimolar mixture of two porphyrins **7** and **8** in overall 75% yield. These two porphyrins were not separated, but used as a mixture in the next step since their reactivities proved to be high with respect to the next Sonogashira cross-coupling reaction.

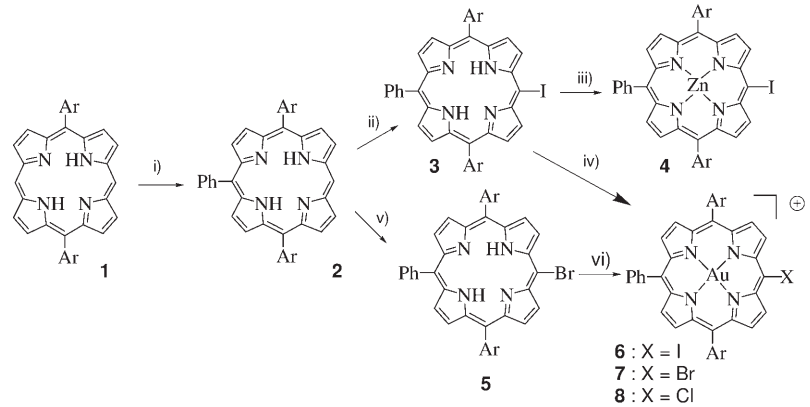

Scheme 3. Synthesis of the porphyrin building blocks. Reagents and conditions: i) 6 equiv PhLi, THF, −78 °C, then H_2O and DDQ (92%); ii) I_2, $(CF_3CO_2)_2IPh$, $CHCl_3$ (99%); iii) $Zn(OAc)_2$, CH_2Cl_2, MeOH (94%); iv) $[Au(tht)_2]SbF_6$, 2,6-lutidine, $CHCl_3$ (38%); v) NBS, CH_2Cl_2, −20 °C to RT. (90%); vi) $HAuCl_4 \cdot 3H_2O$, NaOAc, CH_3CO_2H, 120 °C (75%). DDQ = 2,3-dichloro-5,6-dicyano-1,4-benzoquinone.

Preparation of the spacers: *para*-(Phenyleneethynylene) spacers **19** and **21** were prepared according to the synthetic route reported in Scheme 4. 1-Ethynyl-4-triisopropylsilylethylenyl benzene **11** was easily obtained through two successive Sonogashira cross-coupling reactions starting from commercially available *para*-iodobromobenzene **9**.[22] 1-ethynyl-4-trimethylsilylethylenyl benzene **14** was synthesized from *para*-bromobenzaldehyde **12** starting with a Sonogashira cross-coupling reaction with trimethylsilyl acetylene followed by a Corey–Fuchs reaction with overall 71% yield.[23] Dibromoterephtalic acid was esterified with octanol catalyzed by PTSA (*para*-toluenesulfonic acid) in 87% yield. The last step of the synthesis consists of a double statistical Sonogashira cross-coupling reaction between the bis-halogenophenyl units **16** or **17** and one equivalent of each acetylenic derivative **11** and **14**. The separation of the three products, formed during this reaction, was easily achieved by column chromatography and afforded the desired spacers **18** and **20** in about 50% isolated yield.

Finally, the preparation of the long spacer **23** is described

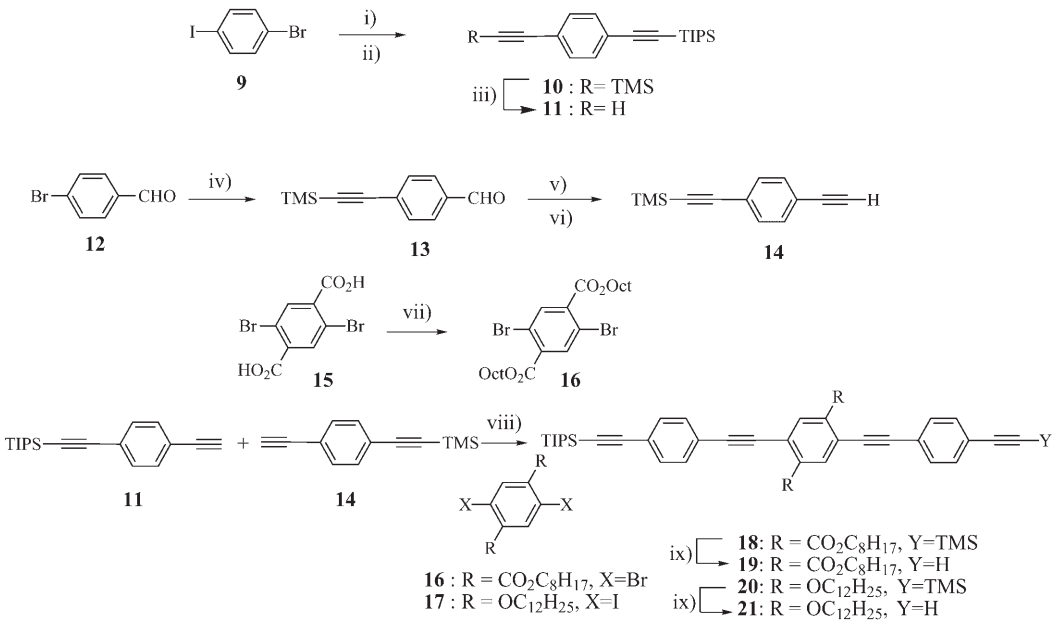

Scheme 4. Synthesis of the *para*-tris(phenyleneethynylene) spacers **19** and **21**. Reagents and conditions : i) trimethylsilylacetylene, PPh_3, CuI, $[Pd_2(dba)_3]$-$CHCl_3$, THF, Et_3N, iPr_2NH, 0 °C, 1 h (98 %); ii) triisopropylsilylacetylene, PPh_3, CuI, $[Pd_2(dba)_3]$-$CHCl_3$, THF, Et_3N, iPr_2NH, 80 °C, 1 h (72 %); iii) K_2CO_3, MeOH, CH_2Cl_2, RT, 1 h (90 %); iv) trimethylsilylacetylene, PPh_3, CuI, $[Pd_2(dba)_3]$-$CHCl_3$, THF, Et_3N, iPr_2NH, 90 °C, 15 h (73 %); v) CBr_4, PPh_3, Zn, CH_2Cl_2, RT, 15 h (100 %); vi) LDA, THF, −80 °C, ½ h then aqueous NH_4Cl, RT, 24 h (98 %); vii) n-OctOH, APTS-H_2O, toluene, 110 °C, 20 h (87 %); viii) PPh_3, CuI, $[Pd_2(dba)_3]$-$CHCl_3$, THF, Et_3N, iPr_2NH, 80 °C, 24 h (41 % for **18** and 55 % for **21**); ix) K_2CO_3, CH_2Cl_2, MeOH, RT (100 %).

in Scheme 5. The iodo dimer partner **22** was obtained by the coupling of **14** with **17** and could be separated from the symmetrical trimer which inevitably formed during this reaction. The elongation of the trimer **21** was then realized by another Sonogashira cross-coupling with **22** in 70 % yield after column chromatography.

The trimethylsilyl protecting group of the spacers **18**, **20**, and **23** was cleaved with potassium carbonate in a quantitative yield (Scheme 6 and 7).

Assembly of the building blocks: The final steps of the synthesis involve connecting the porphyrins to the spacer in a stepwise manner. The zinc iodoporphyrin was first coupled to the spacer, because we observed that the cleavage of the triisopropylsilyl (TIPS) group in presence of the gold porphyrin leads to the formation of by-products, which was not the case with the zinc porphyrin. Most probably, the nucleophilic fluoride anion could react with the electron-deficient gold porphyrin.[24] The zinc iodo porphyrin **4** was therefore reacted with the appropriate spacer using different catalytic systems (phosphine ligands such as tBu_3P, $(oTol)_3P$, $AsPh_3$), but the best conditions found were essentially those initially described by Lindsey and co-workers (Scheme 6).[25]

The deprotection of the triisopropylsilyl group was carried out with tetrabutylammonium fluoride, and the resulting acetylenic derivatives were subjected to the final Sonoga-

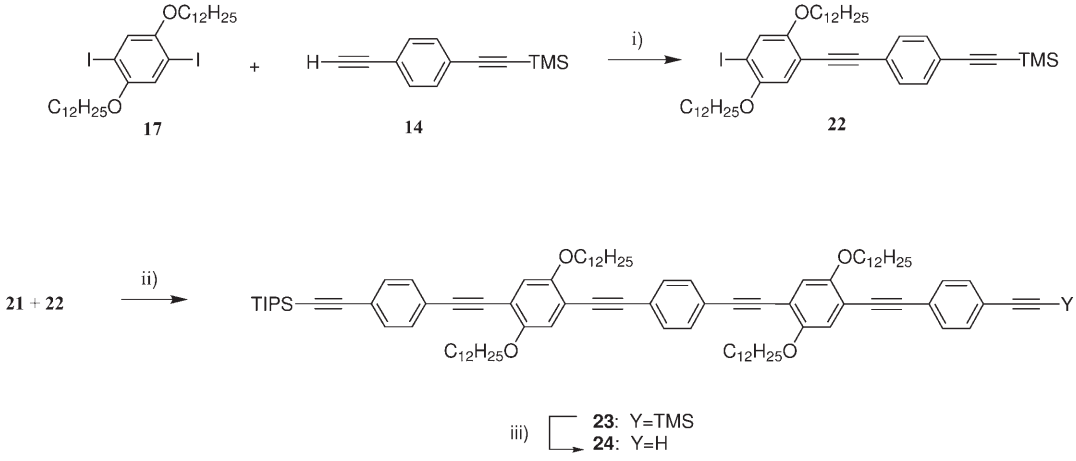

Scheme 5. Synthesis of the spacers **29**. Reagents and conditions: i) PPh_3, CuI, $[Pd_2(dba)_3]$-$CHCl_3$, THF, Et_3N, iPr_2NH, 80 °C, 1 h (25 %); ii) PPh_3, CuI, $[Pd_2(dba)_3]$-$CHCl_3$, THF, Et_3N, iPr_2NH, 80 °C, 12 h (70 %); iii) K_2CO_3, CH_2Cl_2, MeOH, RT (100 %).

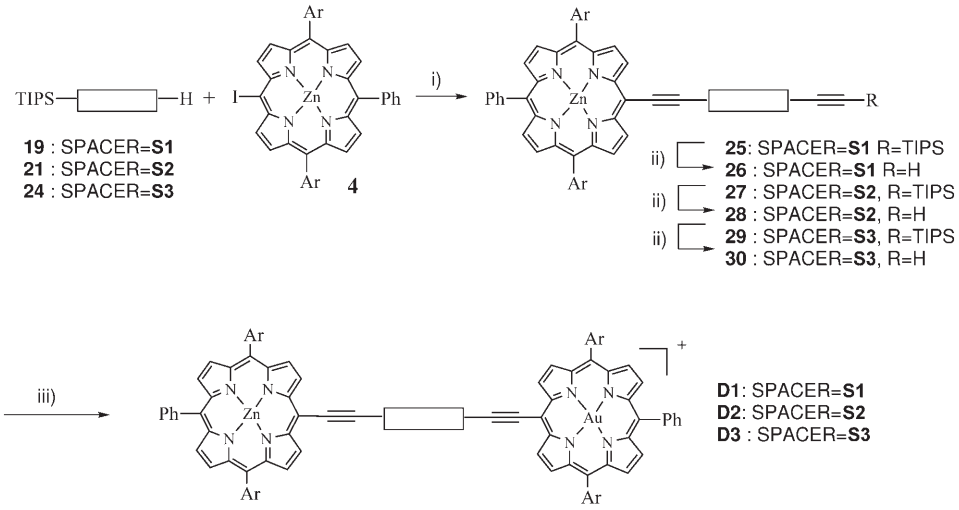

Scheme 6. Synthesis of the dyads **D1**–**D3**. Reagents and conditions: i) $AsPh_3$, $[Pd_2(dba)_3]$-$CHCl_3$, toluene, Et_3N, 60 °C (19–36 %); ii) Bu_4NF, THF, RT (99 %); iii) equimolar **7**:**8**, CuI, $[Pd(dppf)Cl_2]$, Et_3N, DMF, 40–60 °C (50 %)

shira cross-coupling reaction with the mixture of halogenogold porphyrins **7** and **8**. Classical Sonogashira conditions and Lindsey conditions were not suitable for this coupling since they did not afford the expected coupled product.[25] Such phenomena were previously observed with a gold porphyrin substrate by Mårtensson and co-workers.[6b] We found that a $[Pd(dppf)Cl_2]$ catalyst (dppf = diphenylphosphinoferrocene) with copper iodide in a mixture of triethylamine and dimethylformamide proved to be particularly efficient for this coupling, since the two porphyrins **7** and **8** were completely consumed after 5 h at 50 °C and the expected dyads **D1**–**D3** were formed with 50 % yields. During the course of this work, Mårtensson and co-workers reported that the classical catalyst $[Pd_2(dba)_3]$–CH_3Cl (dba = *trans*,*trans*-dibenzylideneacetone) with $AsPh_3$ is active for this type of coupling provided that the polarity of the medium is sufficiently high to ease the deprotonation of the terminal alkyne proton.[26] However, these new conditions were not tested, since they appeared in the literature after the completion of the synthesis of **D1**–**D3.** It is worth noting that the ester groups of spacer **19** tend to hydrolyze during the desylilation and the Sonogashira reactions explaining, thus, the lower yields obtained with the spacer **S1**.

The spacer–AuP^+ systems **31**–**33** were also prepared as references (Scheme 7). The synthesis of these molecules relies on a Sonogashira cross-coupling reaction of the halogenogold porphyrin with the appropriate spacer **S1**–**S3** using the proper catalytic conditions discussed above (Scheme 7).

The porphyrin center-to-center distance in the dyads was estimated by molecular mechanics calculations to be 32 Å for **D1** and **D2** and 45 Å for **D3** (see Supporting Information for synthetic procedures).

Electronic absorption spectra: The UV/Vis absorption spectra of the dyads **D1**–**D3** along with those of the zinc and gold tetraaryl porphyrins are shown in Figure 1 and 2. Table 1 summarizes the absorption data of the porphyrin systems described in this work.

Qualitatively, the spectra of these series of dyads differ from those of the reference tetraaryl porphyrins ZnTdBPP

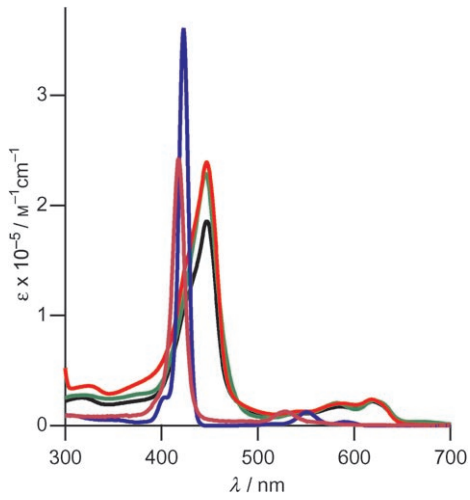

Figure 1. UV/Vis absorption spectra of **D1**–**D3** (black, green, red, respectively), along with those of the tetra(3,5-diterbutylphenyl) zinc(II) (ZnTdBPP; blue) and tetra(3,5-diterbutylphenyl) porphyrin gold(III) ($AuTdBPP^+$; magenta) recorded in dichloromethane.

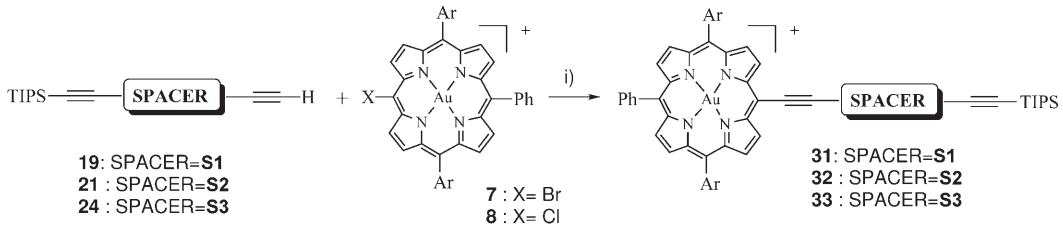

Scheme 7. Synthesis of the reference porphyrin systems **31**–**33**. Reagents and conditions: i) equimolar mixture of **7** and **8**, CuI, $[Pd(dppf)Cl_2]$, Et_3N, DMF, 40–60 °C (40 %).

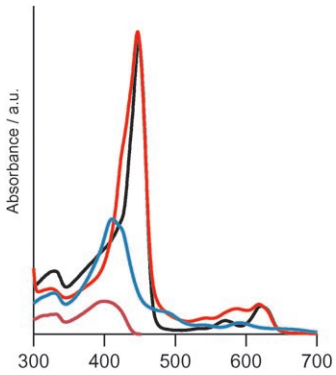

Figure 2. UV/Vis absorption spectrum of **D3** (red) along with those of its components ZnP-S3 (**29**; black), S3-AuP$^+$ (**33**; blue), and **S3** (**24**; magenta) recorded in dichloromethane.

Table 1. UV/Vis absorption data of the compounds recorded in dichloromethane. ZnTdBPP = tetra(3,5-diterbutylphenyl) zinc(II) and AuTdBPP$^+$ = tetra(3,5-diterbutylphenyl)porphyrin gold(III).

Compound	λ_{max} [nm]/ε [$M^{-1}cm^{-1}$]
S2: **20**	256 (3.63×10^4); 275 (2.14×10^4); 323 (6.98×10^4); 384 (7.24×10^4)
ZnP-S2: **27**	323 (8.01×10^4); 380 (6.04×10^4); 446 (5.04×10^5); 570 (2.34×10^4); 620 (4.96×10^4)
AuP-S2: **32**	320 (4.59×10^4); 384 (5×10^4); 424 (1.91×10^5); 540 (1.63×10^4); 587 (2.22×10^4)
D2	317 (2.52×10^4); 447 (1.86×10^5); 545 (1.12×10^4); 586 (1.69×10^4); 619 (2.18×10^4)
S1: **18**	268 (3.61×10^4); 326 (4.21×10^4); 373 (5×10^4)
ZnP-S1: **25**	262 (1.2×10^4); 323 (1.45×10^4); 367 (1.31×10^4); 447 (1.04×10^5); 567 (4.8×10^3); 620 (1.09×10^4)
AuP-S1: **31**	328 (3.25×10^4); 384 (4.16×10^4); 427 (8.9×10^4); 440 (9.84×10^4); 543 (1.14×10^4); 585 (1.56×10^4)
D1	315 (2.77×10^4); 382 (2.93×10^4); 446 (2.29×10^5); 543 (1.28×10^4); 582 (2.07×10^4); 620 (2.28×0^4)
S3: **23**	314 (2.39×10^4); 330 (2.58×10^4); 398 (4.33×10^4)
ZnP-S3: **29**	325 (6.05×10^4); 400 (8.35×10^4); 450 (2.97×10^5); 534 (4.9×10^3); 570 (1.36×10^4); 620 (2.93×10^4)
AuP-S3: **33**	330 (5.2×10^4); 413 (1.41×10^5); 424 (1.54×10^5); 489 (2.65×10^4); 542 (1.33×10^4); 590 (1.91×10^4)
D3	280 (7.39×10^4); 294 (8.65×10^4); 324 (3.6×10^4); 427 (1.54×10^5); 447 (2.41×10^5); 545 (1.29×10^4); 586 (2.03×10^4); 618 (2.38×10^4)
ZnTdBPP	423 (3.13×10^5); 550 (1.32×10^4); 590 (4.3×10^3)
AuTdBPP$^+$	416 (2.57×10^5); 524 (1.26×10^4); 564 (shoulder)

and AuTdBPP$^+$ by a red-shift of the maximum absorption positions of the Soret and Q-transitions and a broadening of the Soret band in particular (Figure 1). The direct attachment of the bridge to the *meso*-position extends the porphyrin π-conjugation, leading to a lower HOMO–LUMO gap and bathochromic absorption shifts. Interaction with the spacer in the ZnP–SX and AuP–SX mono-porphyrinic compounds broadens the Soret band, presumably by splitting the degeneracy of the *x*- and *y*-transitions as observed for other *meso*-ethynyl substituted porphyrins.[7,11,12,27,28] The absorption spectra of the dyads above 400 nm are in good agreement with a sum of the ZnP−SX and AuP−SX components, indicating that the spectrum is not strongly affected by inter-porphyrin interactions. Also, the length of the spacer and the nature of its substituents (alkoxy or ester) have little effect on the electronic transitions of the porphyrin, since the spectra of all three dyads are quite similar in the Soret and Q-bands regions (Figure 1). This indicates that the average conjugation length of the phenyleneethynylene in the ground state is not longer than three ethynylphenylene units. It is important to note that the spacer unit of all the dyads **D1**–**D3** show π–π* absorptions that are blue-shifted relative to the Soret band of the zinc and gold porphyrins (Table 1). This characteristic eliminates the risk of energy transfer from the porphyrin to the spacer.

Electrochemistry: The half-wave redox potentials were determined by square-wave voltammetry (frequency 15 Hz) in dichloromethane and they are collected in Table 2.

Table 2. Redox potentials of the compounds prepared for this study. The electrochemistry was recorded in dichloromethane with 0.15 M of Bu_4NPF_6 as supporting electrolyte and all potentials are reported versus the saturated calomel electrode (SCE). When limiting values are given the process occurred outside the limit of the electroactivity of the electrolyte in our conditions.

	ZnP^+/ZnP [V]	ZnP^{2+}/ZnP^+ [V]	S^+/S [V]	$AuP^+/AuP^\bullet$ [V]	$AuP^\bullet/AuP^-$ [V]	S/S^- [V]
S1: **18**			>1.6			−1.39
ZnP-S1: **25**	0.77	1.20	>1.5			<−1.3
AuP-S1: **31**			>1.5	−0.56	−1.06	<−1.4
D1	0.76	1.16	>1.5	−0.58	−1.05	−1.28
S2: **20**			1.30			<−1.6
ZnP-S2: **27**	0.76	1.18	1.32			<−1.3
AuP-S2: **32**			1.34	−0.56	−1.08	<−1.4
D2	0.74	1.18	>1.4	−0.58	−1.05	
S3: **23**			1.26			<−1.6
ZnP-S3: **29**	0.73	1.14	1.27			<−1.5
AuP-S3: **33**			1.28	−0.57	−1.06	<−1.5
D3	0.74	1.14	1.30	−0.56	−1.05	<−1.5
AuP ref				−0.59	−1.15	
ZnP ref	0.68	1.03				

The zinc porphyrin unit of all new compounds exhibits two oxidation processes that are located around 0.75 V and 1.16 V, respectively. They correspond to the formation of the radical cation and dication on the π-porphyrin ring.[29] The gold porphyrin unit displays a first metal-based reduction at around −0.6 V followed by a porphyrin-based reduction around −1.1 V.[30] The spacers **S2** and **S3** bearing the alkoxy substituents are relatively electron-rich and display similar potentials for oxidation around 1.3 V (Table 2), while their reductions occurred outside the solvent electroactivity window. Conversely, the more electron-deficient spacer **S1** could not be oxidized below 1.6 V, while its potential for reduction could be determined as −1.39 V. Compared to the tetraaryl porphyrins the attachment of the spacer induces an increase of both zinc porphyrin potentials and the second potential of the gold porphyrin. The potentials for oxidation of the spacers in dyads **D2** and **D3** are also anodically shifted by 40 mV compared to the isolated bridges **20** and **23**. These results are consistent with a stabili-

zation of the HOMO and LUMO orbitals of the porphyrin and of the spacers, which is caused by the extended π-conjugation between the spacer and the porphyrins. On the other hand, the negligible shift of the first reduction potential of the gold porphyrin is in agreement with a metal-based process that is naturally less affected by the appended bridge.[32]

Steady-state fluorescence spectroscopy: The steady-state fluorescence spectra of the dyads **D1**–**D3** and the parent compounds ZnP–Spacer **25**, **27**, and **29** were recorded with identical absorbance at the maximum absorption Q-band of the zinc porphyrin.

Both the fluorescence and phosphorenscence spectra are red shifted in the compounds with the spacer attached, compared to zinc and gold tetraaryl porphyrins, in analogy to the absorption spectra. Again, the number of ethynylphenylene units and the nature of the substituents on the spacer play a minor role on the energy of the excited state of the porphyrin units. The zinc porphyrin phosphorescence maximum could not be clearly determined and the triplet energy was estimated to lie 0.46 eV below the corresponding singlet, as for zinc tetraaryl porphyrin. It is noteworthy that the zinc porphyrin fluorescence in all the dyads **D1**–**D3**, is almost completely quenched by the appended gold porphyrin independently of the interporphyrin separation distance (Table 3). In the current dyads, the fluorescence quenching of ZnP originates from intramolecular electron transfer with the gold porphyrin (see below).

Table 3. Emission characteristics of the porphyrins.

	$\lambda_{em}(^1ZnP^*)$ [nm][a]	$E_{00}(^1ZnP^*)$ [eV][b]	$\lambda_{em}(^3MP^*)$ [nm][c]	$E_{00}(^3MP^*)$ [eV][d]	Φ_{em}[e]
ZnP-S1: **25**	635, 689	1.97	n.d.	(1.51)[f]	
AuP-S1: **31**			768	1.61	
D1	634, 691	1.97			0.01
ZnP-S2: **27**	636, 687	1.97	n.d.	(1.51)[f]	
AuP-S2: **32**			768	1.61	
D2	634, 687	1.97			0.02
ZnP-S3: **29**	634, 687	1.97	n.d.	(1.51)[f]	
AuP-S3: **33**			769	1.61	
D3	633, 686	1.97			0.04
AuP ref.				1.82[g]	
ZnP ref.	600, 650	2.10		1.64[g]	

[a] Recorded in dichloromethane at room temperature. [b] Determined from the average of the 0–0 band maxima for absorption and fluorescence. [c] Recorded in ethanol (ZnP) and 2-methyl THF (AuP^+) at 77 K. [d] Determined from the phosphorescence band maximum recorded at 77 K. [e] Φ_{em}: ZnP fluorescence yield in the dyad relative to that of the parent ZnP-SX, in dichloromethane at room temperature. [f] Estimated (see text). [g] From Ref. [13a]

Calculation of the reaction free energy for photoinduced charge separation in the dyads: The redox potentials along with the emission data allow for the determination of the free energy changes of the photoinduced electron transfer from the zinc porphyrin singlet excited state to the gold porphyrin ($\Delta G°_{et}$), of the photoinduced hole transfer from the gold porphyrin triplet excited-state to the zinc porphyrin ($\Delta G°_{ht}$), and finally of the subsequent back electron transfer to reform the ground state reactants ($\Delta G°_{bet}$) As these are charge shift reactions with one uncharged unit in both the reactant and product states, the simplified Rehm-Weller equation (Equations (1)–(3)) could be used (the columbic interaction term equals zero).[31]

$$\Delta G^{\circ}_{ET} = e(E^0(ZnP^+/ZnP) - E^0(AuP^+/AuP) - E_{00}(^1ZnP)) \quad (1)$$

$$\Delta G^{0}_{HT} = e(E^0(ZnP^+/ZnP) - E^0(AuP^+/AuP) - E_{00}(^3AuP^+)) \quad (2)$$

$$\Delta G^{\circ}_{BET} = e(E^0(AuP^+/AuP) - E^0(ZnP^+/ZnP)) \quad (3)$$

Also, the driving force should be independent of solvent polarity for an ideal system in a dielectric continuum, with compensatory charge redistributions on the two porphyrin units. In practice, there may be small differences due to differences in solvation of the $ZnP^{+/0}$ and $AuP^{+/0}$ species.[32]

Time-resolved fluorescence: The fluorescence decays of ZnP references and ZnP/AuP^+ dyads were recorded using a streak camera/spectrograph combination (Hamamatsu, <5 ps fwhm) and 400 nm, 100 fs excitation pulses (see Figure S20 in the Supporting Information). Excitation with 620 nm light yielded the same ZnP lifetimes, but because of the small Stokes shift scattered light contaminated the decays. The fluorescence lifetimes are summarized in Table 5. It should be noted that the measured lifetimes for dyads **D1** and **D2** are comparable to the instrument FWHM, and may possibly be shorter (see transient absorption results below). Compared to the ZnP–SX references, the ZnP emission lifetime in the dyads is strongly reduced in both toluene and dichloromethane. This is consistent with the low relative emission yields in Table 3. A minor component of longer-lived emission is also present, which we tentatively attribute to small quantities of ZnP lacking the AuP moiety remaining after purification, or having formed during irradiation. By combining the fluorescence yield and lifetime data we can conclude that the level of fluorescent impurity is $<2\,\%$ in all dyads.

Table 4. Free energy for electron transfer, hole transfer, and back electron transfer in the dyads **D1**–**D3,** calculated from Equations (1)–(3).

Dyad	$\Delta G°_{ET}$ [eV]	$\Delta G°_{HT}$ [eV]	ΔG^0_{BET} [eV]
D1	−0.63	−0.28	−1.34
D2	−0.65	−0.29	−1.32
D3	−0.67	−0.31	−1.30

Femtosecond transient absorption spectroscopy: Transient spectra after Q-band excitation of the reference compounds

ZnP–S1 and **S1–AuP** in toluene and dichloromethane are shown in Figure 3. The spectra for the other references are virtually identical to those shown, and the dynamics are

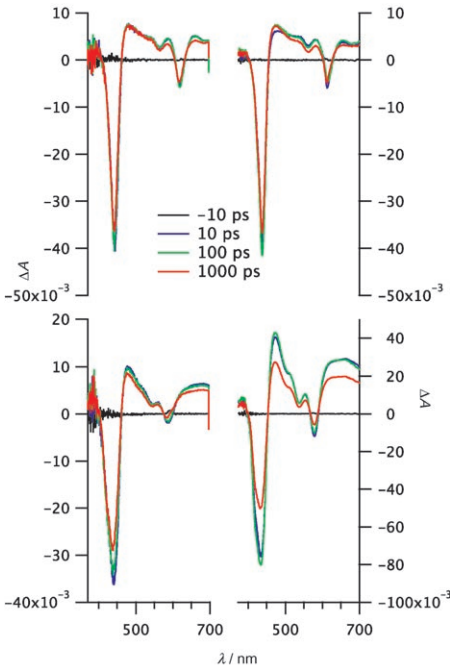

Figure 3. Transient absorption spectra of **ZnP-S1** (top) and **AuP-S1** (bottom) in toluene (left) and dichloromethane (right). The pump wavelength was 620 nm for **ZnP-S1** and 580 nm for **AuP-S1**.

very similar. The initially populated $^1AuP^+$ state of gold porphyrins is known to convert to the lowest $^3AuP^+$ state on a sub-picosecond time scale.[13,33] We observe small-amplitude dynamics on the time scale of a few picoseconds for both the ^{1}ZnP and ^{3}AuP states, tentatively attributed to vibrational and solvent relaxation, but apart from this, the transient spectra decay cleanly. As is typical for Zn-porphyrins, the main decay pathway of the ZnP singlet excited state is intersystem crossing to the long-lived ($\gg$10 ns) ZnP triplet with an observed singlet lifetime of around 2 ns. The Q-band bleaches are distinctly different for the two chromophores, with bleach minima at approximately 565 and 620 nm for ZnP–S1 and at 545 and 585 nm for S1–AuP^+. Also the Soret bleach occurs at somewhat shorter wavelengths for the AuP chromophore. These signatures are useful for interpreting the transient spectra of the dyads below. In line with the thermodynamics for charge and energy transfer, there are no indications that the bridge is involved in any electron or energy transfer reactions in these reference compounds. Interestingly, the ^{3}AuP state is significantly more long-lived (7–10 ns) in toluene than in dichloromethane ($\approx$2 ns). Also, the magnitude of transient absorption above 600 nm is much larger compared to the other features in dichloromethane than in toluene, which was seen also in the dyads below.

In the dyads **D1**–**D3**, we observe multi-exponential transient absorption kinetics following excitation of the ZnP unit as well as the AuP^+ unit, both in toluene and dichloromethane. We analyzed the transient absorption data using a global fitting strategy. The wavelengths were chosen to represent significant spectral features in the bleaching and excited state absorption regions, and to minimize contributions from the solvent. Light-induced electron transfer from the ^{1}ZnP unit and hole transfer from the $^3AuP^+$ unit were observed, both leading to the charge-shifted (CSh) product $ZnP^{\bullet+}$–SX–$AuP^{\bullet}$, as well as subsequent back electron transfer. Kinetic data for these processes are summarized in Table 6.

Table 5. Fluorescence lifetimes of dyads **D1**–**D3** and the corresponding ZnP-SX references.

Dyad	Solvent	τ_f [ps] (τ_f ZnP-SX)
D1	CH_2Cl_2	7 (1800)
D1	toluene	3 (1800)
D2	CH_2Cl_2	6 (1800)
D2	toluene	7 (1800)
D3	CH_2Cl_2	40 (1600)
D3	toluene	390 (1600)

To estimate the expected transient spectrum of the $ZnP^{\bullet+}$–SX–$AuP^{\bullet}$ state, spectroelectrochemistry difference spectra for oxidation of ZnP–SX and reduction of SX–AuP^+ were recorded (see Figure S21 in the Supporting Information). These show mainly bleaching of the ZnP and AuP^+ absorptions. Some new, broad absorption bands appear, due mainly to the $ZnP^{\bullet+}$ species around 480 and 690 nm, but also a narrow difference absorption feature around 460 nm due to the formation of $AuP^{\bullet}$. These additional absorption features are very similar to the excited state features, which is typical for this type of porphyrin.[13] However, inspection of the transient absorption decays reveal the formation of intermediates in the dyads. The spectral changes in the Soret- and Q-band regions show that the intermediate in both ET and HT pathways involves the porphyrin moiety that was not excited (ZnP for HT, AuP^+ for ET pathways). Moreover, the ET intermediate has a transient absorption around 460 nm that is somewhat blue-shifted compared to any of the locally excited states observed, consistent with the CSh state spectrum. Finally, comparison with ^{1}ZnP emission lifetimes allows us to kinetically identify the ET process. Transient absorption traces for **D1** ZnP and AuP excitation are shown in Figure 4, and the associated transient absorption spectra in Figure 5. Additional data is shown in the Supporting Information.

ZnP excitation—high polarity: Electron transfer can be achieved with high selectivity by exciting the ZnP moiety at 620 nm. Careful analysis of the transients obtained for dyads **D1** and **D2** reveals the formation of an intermediate, attributable to the CSh state, with a time constant of 2 ps for both dyads, similar to that for the fluorescence decay (see also Figure S20 in the Supporting Information). The somewhat slower kinetics deduced from the fluorescence experiments

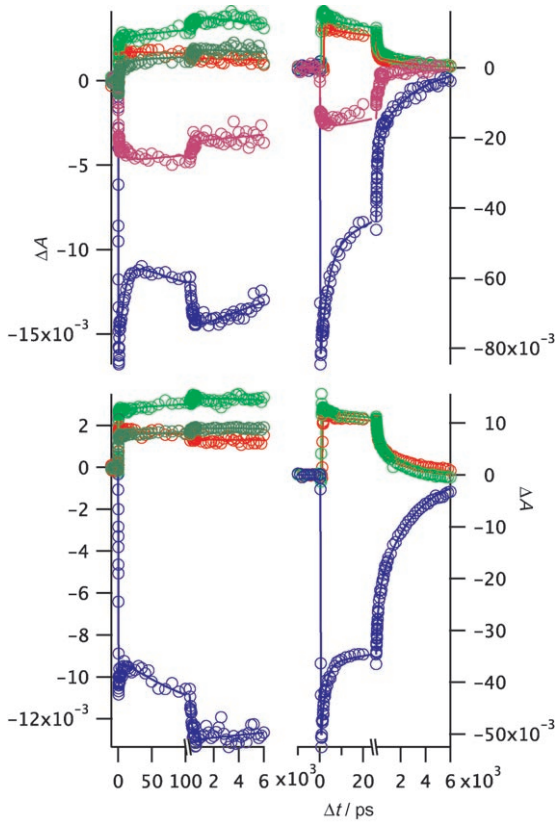

Figure 4. Transient absorption decays for **D1**. Top traces are for excitation of the ZnP unit (620 nm pump), lower traces are for excitation of predominantly the AuP^+ unit (580 nm pump), left traces are in toluene, right traces in dichloromethane. Violet: 422 nm blue: 440 nm, dark green (toluene only): 465 nm, light green: 490 nm, red: 690 nm. Solid lines are best global bi- or triexponential fits to multiple wavelengths. See Supporting Information for corresponding traces for **D2** and **D3.**

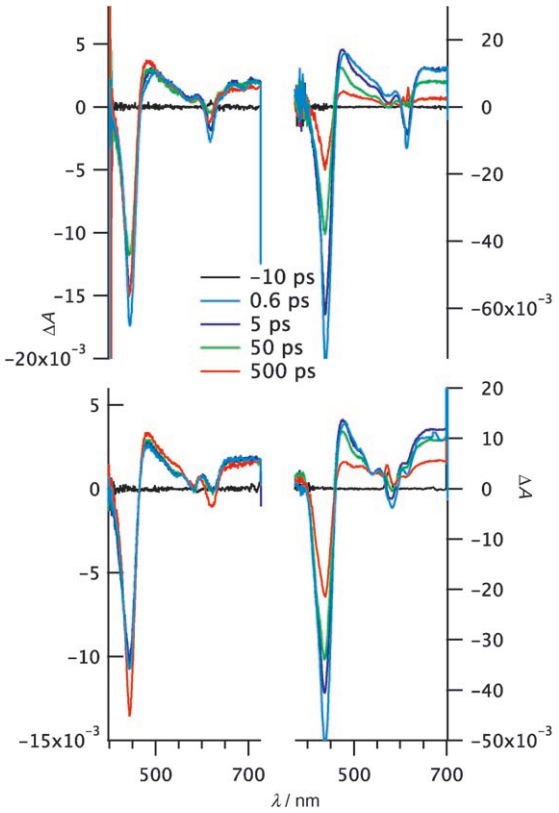

Figure 5. Transient absorption spectra for **D1**. Top spectra are for excitation of the ZnP unit (620 nm pump), lower spectra are for excitation of predominantly the AuP^+ unit (580 nm pump), left spectra are in toluene, right spectra in dichloromethane. Black: −10 ps, light blue: 0.6 ps, violet:5 ps, green:50 ps, red: 500 ps. The 0.6 ps spectrum is chirp-corrected. See Supporting Information for corresponding spectra for **D2** and **D3**.

can be attributed to the limited temporal resolution of the streak camera. The Soret band bleach recovers partially on this time scale, as expected from the spectral differences of the ^{1}ZnP and $ZnP^{\cdot+}$ species. On the blue side, however, there is no recovery because also the AuP^+ transition becomes bleached. Also at the AuP^+ Q-band positions a further bleaching appears. Concomitantly, the absorption feature around 470 nm blue-shifts, and a weak but significant absorption increase is seen at 690 nm, all consistent with formation of the charge-shifted state. Subsequently, the transient features of the CSh state decay with time constants of 90 ps (**D1**) and 80 ps (**D2**), consistent with back electron transfer to reform the ground state reactants. In addition we observe a residual 2–3 ns transient, with a spectrum resembling that of the ZnP triplet, although the lifetime is shorter than expected. The photostability is lower in dichloromethane than in toluene (see below), and the presence of the nanosecond component can be due to degradation. We note that the degree of fluorescent ZnP impurity in the freshly prepared solutions was very low (see above) and cannot account for these signals. Finally, also in the longer dyad **D3** we observe very rapid ET with a time constant of 90 ps, in this case over a 45 Å center-to-center distance. The subsequent back electron transfer is slower, with a time constant of 2.1 ns.

ZnP excitation—low polarity: The results obtained with selective ZnP excitation in toluene are initially very similar to those in dichloromethane. Thus, an intermediate attributable to the CSh state is formed with approximately the same time constant as the fluorescence decay, namely 8 ps for **D1**, and 7 ps for **D2**. This is only slightly slower than in the more polar solvent. For the subsequent back electron transfer the results are instead qualitatively quite different. The CSh state disappears with time constants of 240 ps (**D1**) and 130 ps (**D2**), but the product has the clear spectral characteristics of the ^{3}ZnP state and shows no decay on the time scale of experiment (6 ns). The rise and decay behavior of the signal at 440 nm (Figure 4, top left panel) illustrates clearly the dynamics of the reaction sequence ^{1}ZnP → CSh → ^{3}ZnP, showing that the triplet is indeed formed via the CSh state. By comparison of the ^{1}ZnP–^{3}ZnP absorption difference in the dyad and the reference ZnP–SX, we conclude that the ^{3}ZnP formation is approximately quantitative. Thus the rate of back electron transfer to form the ground state is much slower than the observed reaction leading to the triplet state, and much slower than the back electron transfer in

dichloromethane. Formation of a long-lived ^{3}ZnP state is obviously direct evidence that this state is lower in energy than the CSh state, at least in toluene. In the dyad **D3** the ET reaction is somewhat slower, with a time constant of 370 ps, similar to the fluorescence decay time. As for **D1** and **D2** this is about four times slower than the corresponding process in dichloromethane. The lifetime of the CSh state in **D3** is also comparatively long, around 12 ns. In contrast to the shorter dyads, back electron transfer seems to reform both the ground state and the ^{3}ZnP state in ratio of approximately 2:1 (judging from the ^{3}ZnP signal amplitude).

AuP$^+$ excitation—high polarity: Although not as selective as ZnP excitation, pumping at 590 nm predominantly targets AuP$^+$. This is expected to result in HT from the excited AuP$^+$ to ZnP. Since the singlet excited ^{1}AuP$^+$ undergoes intersystem crossing in a few hundred femtoseconds,[33] the HT rates cannot be determined by our fluorescence measurements. Fortunately, the transient absorption spectra of **D1** show the decay of ^{3}AuP$^+$ and formation of an intermediate species with time constants of 2 ps in both cases, followed by its disappearance with time a constant of 170 ps. The identification of the intermediate as the CSh based on spectral changes is less obvious than with ZnP excitation, partly because the less selective excitation gives some ZnP bleach features already from the beginning. Nevertheless, the blue shift of the 460 nm absorption is seen. As we observe almost total reformation of the ground state much faster than in the SX–AuP$^+$ reference, the dynamics cannot be explained solely by the fraction of ZnP-excited dyads. Also the faster kinetics compared to the reference shows that the reaction of the AuP$^+$-excited dyad involves the ZnP moiety. Finally, this intermediate is observed only in the dyads, it is spectrally different from the ZnP triplet, and the spectra at 20–50 ps are identical to those obtained with ZnP excitation. Thus we assign it to the CSh state formed by HT from ^{3}AuP$^+$. The decay traces on the >100 ps time scale are very similar to those after 620 nm excitation, showing that back electron transfer is rather independent on whether the CSh state was formed from a singlet or triplet excited state (see below). Also, the residual 2–3 ns transient, attributed to partial decomposition, appears just as upon 620 nm excitation above.

In contrast, for **D2** and **D3** we see only small transient amplitude changes with a 2 ps (**D2**) or 23 ps (**D3**) time constant, at least partially due to the fraction of ZnP excitation, but no clear evidence for a CSh state formed from ^{3}AuP$^+$. Instead the spectrum is very similar to the initial ^{3}AuP$^+$ state and decays with a time constant of about 2 ns, very close to the life time of the SX–^{3}AuP$^+$ reference. We see substantial degradation of these dyads with electron-rich bridges during measurements with 590 nm excitation in dichloromethane. Thus, we cannot determine the HT time constants in these cases.

AuP$^+$ excitation—low polarity: In toluene the ^{3}AuP$^+$ is converted to the ^{3}ZnP state with a time constant of 170 ps (**D1**) or 130 ps (**D2**). As in dichloromethane, some dynamics due to ZnP excitation were also observed, but no other intermediates were observed. The magnitude of the ^{3}ZnP signal formed is consistent with quantitative, direct triplet energy transfer from ^{3}AuP$^+$ to ZnP.

In contrast, no energy transfer is observed in the long dyad **D3** in toluene. Only small amplitude dynamics with a roughly 400 ps time constant was observed, attributable to ET from the fraction of ^{1}ZnP created. The main transient appears to be due to the ^{3}AuP$^+$ state decaying with a lifetime of several nanoseconds as in the SX–AuP$^+$ reference.

Discussion of the of charge shift processes: A simplified state energy diagram is given in Figure 6. Formation of the CSh state in dichloromethane is an exergonic process both

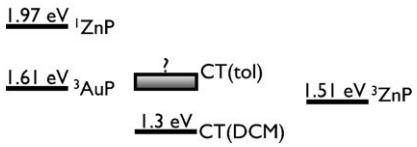

Figure 6. Energies of the excited and charge-shifted states in toluene (tol) and dichloromethane (DCM).

via ET and HT mechanisms, and the ^{3}ZnP state clearly lies above the CSh state. From the discussion around the data in Table 4 one would expect the energetic situation to be very similar in toluene, and it has even been reported that the CSh states of ZnP–AuP$^+$ dyads are stabilized in non-polar solvents.[32] In contrast, we see back electron transfer in toluene that quantitatively forms the ^{3}ZnP state. Thus the CSh state must lie at least 0.2 V higher in toluene than in dichloromethane. The reason could possibly be ion pairing of the AuP$^+$ in toluene so that the effective charge actually increases upon reduction, which would decrease the reduction potential. As the ^{3}ZnP state is estimated to lie only 100 meV below the ^{3}AuP$^+$ state, the lack of HT from the latter in toluene may be because the process has a very weak driving force or is even endergonic.

The very rapid ET and HT processes over several nanometers are remarkable and they are clearly mediated by the bridge. In the super-exchange mechanism virtual states involving the bridge increase the electronic coupling.[2,5,8,18] This can involve either the HOMO or LUMO of the bridge,

Table 6. Time constants from transient absorption experiments. Note that the main product of back electron transfer in toluene is the ^{3}ZnP state, while it is the ground state in dichloromethane.

Dyad	Solvent	ZnP excitation		AuP$^+$ excitation	
		τ_{ET} [ps]	τ_{BET} [ps]	τ_{HT} [ps]	τ_{BET} [ps]
D1	CH_2Cl_2	2	80	2	170
D1	toluene	8	240	(170[a])	
D2	CH_2Cl_2	2	90	[b]	[b]
D2	toluene	7	130	(130[a])	
D3	CH_2Cl_2	85	2100	[b]	[b]
D3	toluene	370	$\approx$12000	[b]	[b]

[a] Time constant for excitation energy transfer from ^{3}AuP$^+$ to ^{3}ZnP. [b] Not observed (see text).

thus defining HT and ET, respectively. Figure 7 shows a relative orbital energy diagram involving the bridges. This is based on the pairing theorem, stating that the HOMO–LUMO energy difference of an organic molecule is equal to the first excitation energy.[34] Thus, for each porphyrin and bridge unit the relative energy for either the HOMO or LUMO is given by the potential for either the first oxidation or first reduction. The other frontier orbital energy is then given by adding or subtracting the singlet excitation energy. This is an approximate procedure, used before for ZnP–AuP$^+$ dyads.[14b] The electrochemical potentials give equilibrium free energy differences for relaxed states, while virtual bridge states are never populated and the relevant energy should be for the geometry of the neutral bridge. Nevertheless, the diagram should be useful to discuss the differences between the dyads and the different processes. First, the diagram shows that charge shift via electron or hole hopping onto the bridge is unlikely, as the bridge states lie approximately 0.3–0.4 eV higher in energy than the electron and hole donor states. Indeed, we measured the activation energy of ET in **D3** in dichloromethane, where the energetics are most in favor of hopping. From the fluorescence lifetime at temperatures between 7 and 34 °C we calculate the activation energy to be very small, only 0.028 eV, which is clearly too low for a hopping mechanism. Since the shorter links disfavor hopping we can conclusively say that ET occurs via superexchange in **D1**–**D3**, and that this probably also holds for HT in **D1**.

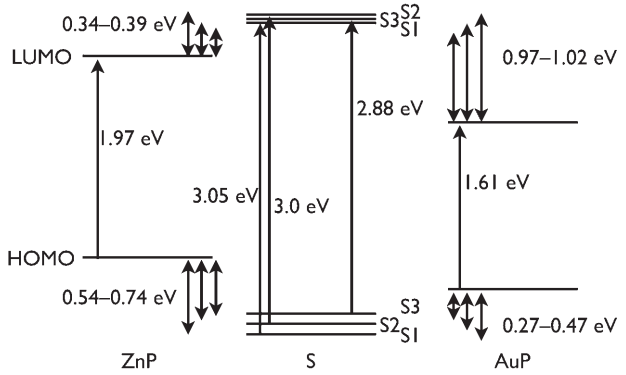

Figure 7. Relative orbital energy diagram of the donor, bridge, and acceptor calculated from redox data in dichloromethane and corresponding E_{00} values.

For a single-step reaction such as these the rate constant (k_{ET}) should follow a Marcus equation for non-adiabatic electron transfer,[8,35] as given in Equation (4), where λ is the reorganization energy and V_{DA} the electronic coupling. The coupling is mediated by the bridge, and is inversely proportional to the energy difference between the donor and bridge states.[2,5,8,16]

$$k_{ET} = \frac{4\pi^2}{h\sqrt{4\pi\lambda k_B T}}|V_{DA}|^2 \exp\left(\frac{-(\Delta G^\circ + \lambda)^2}{4\lambda k_B T}\right) \quad (4)$$

The estimated ZnP–bridge LUMO gap in the present series varies only from 0.34 to 0.39 eV between the electron-rich and electron-deficient bridges (Figure 8). This can explain why we observed no difference for ET in **D1** and **D2**. Also the AuP$^+$–bridge HOMO gaps are similar, and is in fact largest in **D1** where we did observe a very rapid HT. Thus, in the absence of sample decomposition and parallel excitation of the ZnP unit, we would have expected to observe a similarly rapid HT process in **D2.**

We estimate the reorganization energy two ways. First, it is given by Equation (5),[35] where we take the inner reorganization energy λ_i to be 0.2 eV.[13a–d,6a,b]

$$\lambda = \lambda_i + \lambda_o = \lambda_i + \frac{e^2}{4\pi\varepsilon_0}\left(\frac{1}{2R_D} + \frac{1}{2R_A} - \frac{1}{2R_{DA}}\right)\left(\frac{1}{n^2} - \frac{1}{\varepsilon_s}\right) \quad (5)$$

For the dyads **D1**–**D3**, using $R_D = R_A = 4.8$ Å, $R_{CC} = 33$ Å for **D1** and **D2**, and $R_{CC} = 45$ Å for **D3**, in dichloromethane we estimate the total reorganization energy to be about 1.2 eV. For the charge shift via the ET mechanism in **D3**, $\Delta G^0 = -0.67$ eV. From these values we predict an activation energy of 58 meV, which is close to the observed value of 28 meV above. Starting instead from the experimental activation energy and driving force, Equation (4) gives a value of $\lambda = 1.0$ eV Using the value of 28 meV in Equation (4) we estimate the electronic coupling to be about 150 cm^{-1} for ET in **D1** and **D2**, and about 20 cm^{-1} in **D3**.

It may be surprising that the rates of ET and HT for **D1** in dichloromethane are very similar, as the driving force for HT is much smaller, $\Delta G^0 = -0.28$ eV. The close similarity in rate is however typical for ZnP–AuP$^+$ dyads.[13] As the reorganization energy is not expected to be significantly different for ET and HT, this implies that a stronger electronic coupling for the HT process compensates for the smaller driving force. However, the origin of stronger coupling is not easily rationalized by inspection of frontier orbitals, (see Ref. [14b]). With $\lambda = 1.0$–1.2 eV the predicted activation energy for HT is 0.13–0.18 eV, and Equation (4) implies a coupling that is four to ten times that for ET. While this is not impossible, we note that already the coupling strength estimated for ET puts this reaction on the limit of an adiabatic reaction. For a solvent-controlled adiabatic electron transfer reaction the pre-exponential factor of Equation (4) should be replaced by $(16\pi k_b T/\lambda)^{1/2}/\tau_L$, which for $\lambda \approx 1.0$ eV at room temperature becomes $\approx 1/\tau_L$.[8] Thus, the reaction rate is then controlled by the longitudinal relaxation time of the solvent rather than by the electronic coupling. We note that the time constants for ET and HT in **D1** are very close to the solvent relaxation times obtained by dynamic Stokes shift measurement: $<\tau> = 0.56$ ps for dichloromethane and $<\tau> = 2.72$ ps for toluene.[36] Finally, the rapid ET and HT reactions in **D1** and **D2** occur on a time scale comparable to relaxation observed in the reference compounds. To conclude, Equation (4) may not be perfectly valid in these cases, which may explain why the difference in driving force for ET and HT does not result in significantly different rates.

With this in mind, the somewhat slower ET in toluene than in dichloromethane could be due to slower solvent dynamics, and/or due to a higher free energy of activation. The reorganization energy should be very small in toluene as $n^2 \approx \varepsilon_s$[36] ([Eq. (2)]) so that ET occurs in the Marcus inverted region, but at the same time the driving force is smaller than in dichloromethane. We can not estimate these parameters for toluene with meaningful precision, but as the activation energy is very small in dichloromethane it is likely to be higher in toluene.

Back electron transfer (BET) is much slower than solvent controlled and should follow the non-adiabatic Equation (4). It is slower in toluene than in dichloromethane, and as the main product is ^{3}ZnP, BET to the ground state is even slower. This is most readily explained by the low reorganization energy in toluene that puts BET to the ground state far into the inverted region. In dichloromethane instead BET to the ground state should be near activationless, based on the parameter estimates above. BET to form a triplet excited chromophore is a phenomenon observed also in photosynthetic reaction centers, and it has been investigated and successfully exploited in a series of papers by Wasielewski and coworkers.[37] This opens up the possibility of controlling the product formation, and also the lifetime, of the product, using the polarity of the medium in which the photoinduced reaction takes place. One application could be to use the long-lived ZnP triplet as a reservoir for photon energy if the energy levels can be tuned so that the triplet-charge-shift gap is small. Unfortunately, the solubilities of the dyads preclude a more comprehensive investigation of the solvent dependence in the present dyads.

While ET would result in a singlet CSh state, HT from ^{3}AuP$^+$ should form the corresponding triplet state. While the subsequent BET in **D1** is somewhat slower upon AuP$^+$ excitation (170 ps, versus 80 ps after ZnP excitation) the difference is not dramatic and given the complexity of data analysis perhaps not significant. Thus, it seems that the presence of the heavy gold ion induces sufficient singlet–triplet mixing in the CSh state to make spin effects negligible, as has been observed before.

It is further interesting to compare the rate constants for ET and back electron transfer (BET) in this strongly coupled system with data from other ZnP–AuP$^+$ dyads. The rate constant for ET in **D1**–**D3** is 20–40 times larger than for BET, which is a favorable property for efficient and yet long-lived photoinduced charge separation, and is a long-standing target of artificial photosynthesis. These values seems to be typical for a range of published ZnP–AuP$^+$ dyads with very different bridges and geometries, which all give a k_{ET}/k_{BET} ratio of 10–100.[13,14] The strong coupling obtained by direct coupling of the ethynyl group to the porphyrin *meso*-position obviously gives a similar effect for the excited state ET and HT reaction as for the ground state BET.

Albinsson and co-workers have made extensive, quantitative investigations of bridge-mediated electron transfer in bis-porphyrins.[6,14] In Figure 8 we plot the rate constants for

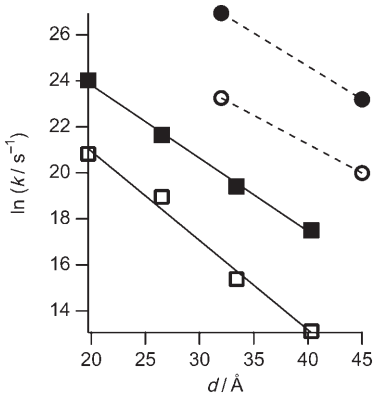

Figure 8. Distance dependence for ET and BET in the present dyads (circles) and those of reference [14b] (squares). Solid lines are best linear fits, with slopes (-β) of −0.31 (ET) and −0.39 (BET). Filled symbols: ET from ^{1}ZnP to AuP$^+$; open symbols: BET from the charge shifted state to form the ground state. Dashed lines are a visual aid.

ET and BET as a function of distance in a series of ZnP–AuP$^+$ dyads, linked by oligo-ethynylphenylene bridges via a *meso*-phenyl group of the porphyrins.[14b] For comparison, we also plot our data for the present series of dyads in dichloromethane. The important structural difference between the series is that **D1**–**D3** are linked with an ethynyl group directly on the porphyrin core. The effect on the observed rate is dramatic, with rates three orders of magnitude larger for both ET and BET in **D1**–**D3**. As Albinsson and co-workers estimated activation energies very similar to ours, the effect is due to a much stronger electronic coupling in our dyads. Rotation of the cylindrically symmetric π-system of polyethynyls should not alter the electronic coupling. Thus, the main mechanism for reducing the coupling in oligo-ethynylphenylenes is probably rotation of the phenyls. If we compare data for dyads of the two series in Figure 8 that have the same number of phenyl groups between the porpyrin cores (that is, **D1** and **D2** with the points at 26.5 Å in the lower series, and **D3** with the points at 40.3 Å) we still find that the rates are about two orders of magnitude higher in **D1**–**D3**. A possible rationale for this is the hindered rotation of *meso*-phenyl groups in the weakly coupled system, which for steric reasons prefer to be oriented orthogonally to the porphyrin plane.[6,14,16] This is probably the main decoupling factor as rotation of the other phenyls should be unhindered. It is obvious from the perturbed ground state properties that the direct ethynyl link couples the bridge very strongly to the porphyrin, and the excited and radical states are most likely partially delocalized onto the bridge.[11,12,27a] As discussed above, however, the ground state perturbation does not seem to extend beyond three ethynylphenylene units. In line with this observation, the rate constants for ET and BET decrease about as steeply with distance between **D1**/**D2** and **D3** as in the more weakly coupled series of Reference [14b]. This may suggest that while ET in the shorter dyads is on the adiabatic limit, ET in **D3** and BET in all dyads follow the exponential decrease of rate with distance as expected for weakly coupled systems

(non-adiabatic reaction). With only two data points, and ET rates similar to those for excited state relaxation, we refrain from reporting β values for our systems.

It has recently been pointed out that OPE linkers are not as rigid as they may appear.[38] However, even in view of these results, thermal fluctuations at room temperature should change the end-to-end distance of the bridge by less than 10%. Since the donor–acceptor coupling at these distances is entirely through-bond, rotation of the phenylene and pophyrin planes are likely to give a much larger effect. In principle the bending fluctuations will also affect the energy of the bridge, but as the D–B and B–A energy gap is much larger than kT we believe that the effect is negligible.

Conclusions

We have reported the synthesis of three new porphyrin dyads consisting of a zinc porphyrin linked to a gold porphyrin via a long and rigid conjugated spacer anchored directly on the *meso* position through an ethynylene group. These new systems exhibit strong porphyrin-bridge electronic coupling as evidenced by absorption and emission spectra and electrochemical potentials. This leads to very rapid electron and hole transfer processes upon light excitation of one of the porphyrin units. The rate constants for these processes are two to three orders of magnitude higher than for very similar ZnP–AuP$^+$ dyads linked via *meso*-phenyl groups. These results give evidence for highly efficient electron transfer mediation by the oligo(ethynylphenylene) spacers when they are directly connected to the porphyrin ring via a triple bond, since very rapid electron transfer can be achieved over distances as long as 45 Å. We[11] and others[27a] have previously reported ET from ethenylphenylene-bridged Zn-porphyrin-acceptor systems, but although the bridge was much shorter the rates were slower than for **D1** and **D2** of the present study. Our results also underscore the utility of connecting a conjugated spacer directly on the porphyrin core to develop porphyrin arrays for long-distance photoinduced charge separation (see Ref [7]). This result opens up new design strategies for vectorial electron transfer over very long distances with porphyrin systems, with a view to applications for solar energy transformations and molecular electronics.

Acknowledgements

We gratefully acknowledge financial support for this project from The French Research Ministry through the programs "ACI Jeune Chercheur" and the ANR blanc "PhotoCumElec", The Swedish Foundation for Strategic Research, The K&A Wallenberg Foundation, The Swedish Energy Agency and The European Commission (COST D35).

[1] V. Balzani, P. Piotrowiak, M. A. J. Rodgers, J. Mattay, D. Astruc, H. B. Gray, J. Winkler, S. Fukuzumi, T. E. Mallouk, Y. Haas, A. P. de Silva, I. Gould, *Electron Transfer in Chemistry*, Wiley-VCH, Weinheim, **2001**.

[2] V. Balzani, F. Scandola, *Supramolecular Photochemistry*, Ellis Horwood, Chischester, **1991**.

[3] a) M. R. Wasielewski, *Chem. Rev.* **1992**, *92*, 435–461; b) D. Gust, T. A. Moore, A. L. Moore, *Acc. Chem. Res.* **1993**, *26*, 198–205; c) D. Gust, T. A. Moore, A. L. Moore, S. J. Lee, E. Bittersmann, D. K. Luttrull, A. A. Rehms, J. M. DeGraziano, X. C. Ma et al., *Science* **1990**, *248*, 199–201; d) J. H. Alstrum-Acevedo, M. K. Brennaman, T. J. Meyer, *Inorg. Chem.* **2005**, *44*, 6802–6824; e) E. Baranoff, J.-P. Collin, L. Flamigni, J.-P. Sauvage, *Chem. Soc. Rev.* **2004**, *33*, 147–155.

[4] a) D. M. Guldi, H. Imahori, K. Tamaki, Y. Kashiwagi, H. Yamada, Y. Sakata, S. Fukuzumi, *J. Phys. Chem. A* **2004**, *108*, 541–548; b) H. Imahori, Y. Sekiguchi, Y. Kashiwagi, T. Sato, Y. Araki, O. Ito, H. Yamada, S. Fukuzumi, *Chem. Eur. J.* **2004**, *10*, 3184–3196; c) H. Imahori, Y. Sekiguchi, Y. Kashiwagi, T. Sato, Y. Araki, O. Ito, H. Yamada, S. Fukuzumi, *Chem. Eur. J.* **2004**, *10*, 3184 –3196; d) H. Imahori, K. Tamaki, D. M. Guldi, C. Luo, M. Fujitsuka, O. Ito, Y. Sakata, S. Fukuzumi, *J. Am. Chem. Soc.* **2001**, *123*, 2607–2617.

[5] W. B. Davis, M. A. Ratner, M. R. Wasielewski, *J. Am. Chem. Soc.* **2001**, *123*, 7877–7886; W. B. Davis, W. A. Svec, M. A. Ratner, M. R. Wasielewski, *Nature* **1998**, *396*, 60–63; R. T. Hayes, M. R. Wasielewski, D. Gosztola, *J. Am. Chem. Soc.* **2000**, *122*, 5563–5567.

[6] a) K. Pettersson, J. Wiberg, T. Ljungdahl, J. Mårtensson, B. Albinsson, *J. Phys. Chem. B* **2006**, *110*, 319–326; b) K. Kilsa, J. Kajanus, A. N. Macpherson, J. Mårtensson, B. Albinsson, *J. Am. Chem. Soc.* **2001**, *123*, 3069–3080; c) ; K. Kilsa, J. Kajanus, S. Larsson, A. N. Macpherson, J. Mårtensson, B. Albinsson, *Chem. Eur. J.* **2001**, *7*, 2122–2133; d) M. U. Winters, K. Pettersson, J. Mårtensson, B. Albinsson, *Chem. Eur. J.* **2005**, *11*, 562–573.

[7] M. U. Winters, E. Dahlstedt, H. E. Blades, C. J. Wilson, M. J. Frampton, H. L. Anderson, B. Albinsson, *J. Am. Chem. Soc.* **2007**, *129*, 4291–4297.

[8] a) *Molecular Electronics* (Eds.: J. Jortner, M. Ratner), Blackwell, London, **1997**; b) M. Bixon, J. Jortner, *Adv. Chem. Phys.* **1999**, *106*, 35–202; c) P. F. Barbara, T. J. Meyer, M. A. Ratner, *J. Phys. Chem.* **1996**, *100*, 13148–13168.

[9] a) F. Giacalone, J. L. Segura, N. Martin, J. Ramey, D. M. Guldi, *Chem. Eur. J.* **2005**, *11*, 4819–4834; b) S. A. Vail, P. J. Krawczuk, D. M. Guldi, A. Palkar, L. Echegoyen, J. P. C. Tome, M. A. Fazio, D. I. Schuster, *Chem. Eur. J.* **2005**, *11*, 3375–3388; c) F. Giacalone, J. L. Segura, N. Martin, D. M. Guldi, *J. Am. Chem. Soc.* **2004**, *126*, 5340–5341; d) G. De La Torre, F. Giacalone, J. L. Segura, N. Martin, D. M. Guldi, *Chem. Eur. J.* **2005**, *11*, 1267–1280.

[10] a) F. Odobel, F. Suzenet, E. Blart, J.-P. Quintard, *Org. Lett.* **2000**, *2*, 131–133; b) E. Blart, F. Suzenet, J.-P. Quintard, F. Odobel, *J. Porphyrins Phthalocyanines* **2003**, *7*, 207–213.

[11] C. Monnereau, J. Gomez, E. Blart, F. Odobel, S. Wallin, A. Fallberg, L. Hammarström, *Inorg. Chem.* **2005**, *44*, 4806–4817.

[12] F. Odobel, S. Suresh, E. Blart, Y. Nicolas, J.-P. Quintard, P. Janvier, J.-Y. Le Questel, B. Illien, D. Rondeau, P. Richomme, T. Haupl, S. Wallin, L. Hammarström, *Chem. Eur. J.* **2002**, *8*, 3027–3046.

[13] a) A. M. Brun, A. Harriman, V. Heitz, J. P. Sauvage, *J. Am. Chem. Soc.* **1991**, *113*, 8657–8663; b) A. M. Brun, S. J. Atherton, A. Harriman, V. Heitz, J. P. Sauvage, *J. Am. Chem. Soc.* **1992**, *114*, 4632–4639; c) J. C. Chambron, A. Harriman, V. Heitz, J. P. Sauvage, *J. Am. Chem. Soc.* **1993**, *115*, 6109–6114; d) A. Harriman, V. Heitz, J. C. Chambron, J. P. Sauvage, *Coord. Chem. Rev.* **1994**, *132*, 229–234; e) A. Harriman, V. Heitz, J. P. Sauvage, *J. Phys. Chem.* **1993**, *97*, 5940–5946; f) J. C. Chambron, S. Chardon-Noblat, A. Harriman, V. Heitz, J. P. Sauvage, *Pure Appl. Chem.* **1993**, *65*, 2343–2392; g) J. C. Chambron, A. Harriman, V. Heitz, J. P. Sauvage, *J. Am. Chem. Soc.* **1993**, *115*, 7419–7425; h) J.-P. Collin, A. Harriman, V. Heitz, F. Odobel, J.-P. Sauvage, *J. Am. Chem. Soc.* **1994**, *116*, 5679–5690; i) L. Flamigni, I. M. Dixon, J.-P. Collin, J.-P. Sauvage, *Chem. Commun.* **2000**, 2479; j) I. M. Dixon, J.-P. Collin, J.-P. Sauvage, L. Flamigni, *Inorg. Chem.* **2001**, *40*, 5507–5517; k) M. Andersson, M. Linke, J.-C. Chambron, J. Davidsson, V. Heitz, J.-P. Sauvage, L. Hammarström, *J. Am. Chem. Soc.* **2000**, *122*, 3526–3527; l) M. An-

dersson, M. Linke, J.-C. Chambron, J. Davidsson, V. Heitz, L. Hammarström, J.-P. Sauvage, *J. Am. Chem. Soc.* **2002**, *124*, 4347–4362.
[14] a) J. Andreasson, G. Kodis, T. Ljungdahl, A. L. Moore, T. A. Moore, D. Gust, J. Mårtensson, B. Albinsson, *J. Phys. Chem. A* **2003**, *107*, 8825–8833; b) J. Wiberg, L. Guo, K. Pettersson, D. Nilsson, T. Ljungdahl, J. Mårtensson, B. Albinsson, *J. Am. Chem. Soc.* **2007**, *129*, 155–163.
[15] a) M. J. Crossley, P. J. Sintic, J. A. Hutchison, K. P. Ghiggino, *Org. Biomol. Chem.* **2005**, *3*, 852–865; b) K. Ohkubo, P. J. Sintic, N. V. Tkachenko, H. Lemmetyinen, W. E. Z. Ou, J. Shao, K. M. Kadish, M. J. Crossley, S. Fukuzumi, *Chem. Phys.* **2006**, *326*, 3–14.
[16] M. P. Eng, B. Albinsson, *Angew. Chem.* **2006**, *118*, 5754–5757; *Angew. Chem. Int. Ed.* **2006**, *45*, 5626–5629.
[17] a) P. F. H. Schwab, M. D. Levin, J. Michl, *Chem. Rev.* **1999**, *99*, 1863–1934; b) U. H. F. Bunz, *Chem. Rev.* **2000**, *100*, 1605–1644; c) R. E. Martin, F. Diederich, *Angew. Chem. Int. Ed.* **1999**, *38*, 1351–1377; d) J. M. Tour, J. S. Schumm, D. L. Pearson, *Angew. Chem.* **1994**, *106*, 1445–1448; *Angew. Chem. Int. Ed. Engl.* **1994**, *33*, 1360–1363; e) J. M. Tour, *Acc. Chem. Res.* **2000**, *33*, 791–804; f) Y. Zhao, Y. Shirai, A. D. Slepkov, L. Cheng, L. B. Alemany, T. Sasaki, F. A. Hegmann, J. M. Tour, *Chem. Eur. J.* **2005**, *11*, 3643–3658.
[18] a) M. O. Senge, *Acc. Chem. Res.* **2005**, *38*, 733–743; b) M. O. Senge, W. W. Kalisch, I. Bischoff, *Chem. Eur. J.* **2000**, *6*, 2721–2738; c) X. Feng, M. O. Senge, *J. Chem. Soc. Perkin Trans. 1* **2001**, 1030–1038.
[19] R. W. Boyle, C. K. Johnson, D. Dolphin, *J. Chem. Soc. Chem. Commun.* **1995**, 527–528.
[20] J. C. Chambron, V. Heitz, J. P. Sauvage, *New J. Chem.* **1997**, *21*, 237–240.
[21] a) E. B. Fleischer, A. Laszlo, *Inorg. Nucl. Chem. Lett.* **1969**, *5*, 373–376; b) J. W. Buchler, *Synthesis and properties of metalloporphyrins, Vol. 1*, Academic Press, New York, **1978**.
[22] A. Godt, *J. Org. Chem.* **1997**, *62*, 7471–7474.
[23] J.-F. Nierengarten, S. Zhang, A. Gegout, M. Urbani, N. Armaroli, G. Marconi, Y. Rio, *J. Org. Chem.* **2005**, *70*, 7550–7557.
[24] H. Segawa, R. Azumi, T. Shimidzu, *J. Am. Chem. Soc.* **1992**, *114*, 7564–7565.
[25] R. W. Wagner, T. E. Johnson, F. Li, J. S. Lindsey, *J. Org. Chem.* **1995**, *60*, 5266–5273.
[26] T. Ljungdahl, K. Pettersson, B. Albinsson, J. Mårtensson, *J. Org. Chem.* **2006**, *71*, 1677–1687.
[27] a) N. P. Redmore, I. V. Rubtsov, M. J. Therien, *J. Am. Chem. Soc.* **2003**, *125*, 8769–8778; b) S. M. LeCours, S. G. DiMagno, M. J. Therien, *J. Am. Chem. Soc.* **1996**, *118*, 11854–11864; c) R. Shediac, M. H. B. Gray, H. T. Uyeda, R. C. Johnson, J. T. Hupp, P. J. Angiolillo, M. J. Therien, *J. Am. Chem. Soc.* **2000**, *122*, 7017–7033.
[28] a) H. L. Anderson, *Chem. Commun.* **1999**, 2323–2330; b) H. L. Anderson, *Inorg. Chem.* **1994**, *33*, 972.
[29] a) R. H. Felton, *Primary redox reactions of metalloporphyrins, Vol. 5*, Academic Press, New York, **1978**; b) A. Wolberg, J. Manassen, *J. Am. Chem. Soc.* **1970**, *92*, 2982–2991; c) J. Fajer, D. C. Borg, A. Forman, D. Dolphin, R. H. Felton, *J. Am. Chem. Soc.* **1970**, *92*, 3451–3459.
[30] Z. Ou, K. M. Kadish, W. E. J. Shao, P. J. Sintic, K. Ohkubo, S. Fukuzumi, M. J. Crossley, *Inorg. Chem.* **2004**, *43*, 2078–2086.
[31] D. Rehm, A. Weller, *Isr. J. Chem.* **1970**, *8*, 259–271; A. Weller, *Z. Phys. Chem.* **1982**, *133*, 93–98.
[32] S. Fukuzumi, K. Ohkubo, W. O. E, Z. , J. Shao, K. M. Kadish, J. A. Hutchison, K. P. Ghiggino, P. J. Sintic, M. J. Crossley, *J. Am. Chem. Soc.* **2003**, *125*, 14984–14985.
[33] a) J. Andreasson, G. Kodis, S. Lin, A. L. Moore, T. A. Moore, D. Gust, J. Mårtensson, B. Albinsson, *Photochem. Photobiol.* **2002**, *76*, 47–50; b) M. P. Eng, T. Ljungdahl, J. Andreasson, J. Mrtensson, B. Albinsson, *J. Phys. Chem. A* **2005**, *109*, 1776–1784.
[34] W. B. Davis, M. A. Ratner, M. R. Wasielewski, *Chem. Phys.* **2002**, *281*, 333–346.
[35] R. A. Marcus, N. Sutin, *Biochim. Biophys. Acta Rev. Bioenerg.* **1985**, *811*, 265–322.
[36] a) L. Reynolds, J. A. Gardecki, S. J. V. Frankland, M. L. Horng, M. Maroncelli, *J. Phys. Chem.* **1996**, *100*, 10337–10354; b) M. L. Horng, J. A. Gardecki, A. Papazyan, M. Maroncelli, *J. Phys. Chem.* **1995**, *99*, 17311–17337.
[37] a) K. Hasharoni, H. Levanon, S. R. Greenfield, D. J. Gosztola, W. A. Svec, M. R. Wasielewski, *J. Am. Chem. Soc.* **1995**, *117*, 8055–8056; b) M. R. Wasielewski, *J. Org. Chem.* **2006**, *71*, 5051–5066, and references therein.
[38] a) A. Godt, M. Schulte, H. Zimmermann, G. Jeschke, *Angew. Chem.* **2006**, *118*, 7722–7726; *Angew. Chem. Int. Ed.* **2006**, *45*, 7560–7564; b) B. D. Allen, A. C. Benniston, A. Harriman, L. J. Mallon, C. Pariani, *Phys. Chem. Chem. Phys.* **2006**, *8*, 4112–4118.

Received: August 27, 2007
Published online: February 12, 2008

